ACS Macro Letters

Letter

pubs.acs.org/macroletters

Rationally Engineering Dual Missions in One Statistical Copolymer Nanocapsule: Bacterial Inhibition and Polycyclic Aromatic Hydrocarbon Capturing

Qingrui Geng,[†,‡] Jiangang Xiao,[‡] Bo Yang,[‡] Tao Wang,[‡] and Jianzhong Du*[,†,‡]

[†]Shanghai Tenth People's Hospital, Tongji University School of Medicine, 301 Middle Yanchang Road, Shanghai 200072, China

[‡]School of Materials Science and Engineering, Key Laboratory of Advanced Civil Engineering Materials of Ministry of Education, Tongji University, 4800 Caoan Road, Shanghai 201804, China

Supporting Information

ABSTRACT: Effective inhibition of bacteria and removal of carcinogenic organic pollutants such as polycyclic aromatic hydrocarbons (PAHs) are important technical challenges in water purification because most of the traditional filter membranes are prone to being biologically contaminated by bacteria and difficult to filter off PAHs. Herein we present the synthesis and characterization of a novel multifunctional nanocapsule (vesicle) based on a *statistical* copolymer, poly[[2-hydroxy-3-(naphthalen-1-ylamino)propyl methacrylate]-*stat*-[2-(*tert*-butylamino)ethyl methacrylate]] [P(HNA$_{23}$-*stat*-TA$_{20}$)], which can be easily synthesized in one step. The TA moiety is engineered for effective bacterial inhibition, while the HNA moiety is in charge of the capturing of PAHs by $\pi-\pi$ stacking. The nanocapsules can effectively inhibit bacteria and quickly reduce the pyrene content in water to an extremely low residual concentration of 5.6 (in 1 min) or 0.56 (in 60 min) parts per billion (ppb). Moreover, this rational engineering principle could be extended by statistically copolymerizing HNA with other functional monomers for designing a range of multifunctional nanomaterials.

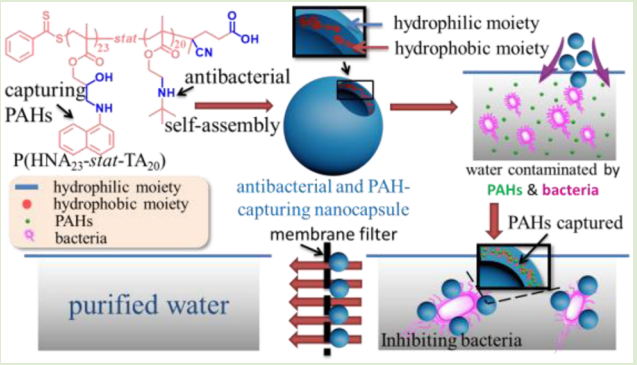

Water remediation is an important global problem because it is closely related to human lives. Among all the issues in water remediation, inhibition of bacteria in water is very important because some pathogenic bacteria may cause many dangerous diseases,[1−6] even some cancers.[7,8] Traditionally, many kinds of membranes were used as filters to treat bacteria in water.[9,10] However, bacteria are prone to causing biofouling via the formation of biofilms in filter membranes, resulting in the blocking of pores in the membranes and thus reducing the filtration ability.[11,12] Therefore, it is necessary to inhibit the bacteria growth before water passes through the filter. Poly[2-(*tert*-butylamino)ethyl methacrylate] (PTA) is a polycationic substance with high antibacterial activity and low toxicity to human cells without antibiotic resistance.[13] Its *tert*-butylamino groups in the PTA can exchange with Ca^{2+} or/and Mg^{2+} in the outer membrane of bacteria, which will cause the disorganization of the membrane and the lysis of cells and result in the death of bacteria.[14,15] Moreover, we recently found that antibacterial polymers in their self-assembled state (such as micelles and vesicles) exhibited much better antibacterial activities than the individual antibacterial polymer chains because of increased local cationic charges in the self-assembled state.[5,16−19]

Polycyclic aromatic hydrocarbons (PAHs) capturing is another important problem in water remediation due to their high toxicity, mutagenicity, and carcinogenicity.[20−24] Although the solubility of PAHs is low in water, PAHs are strongly bioaccumulative and may affect people through food chain transfer.[25,26] In practice, low cost adsorbents (such as activated carbon) are used to remove PAHs, while they are weak in affinity because of its rigid structure.[27] In contrast, organic adsorbents have better efficiency in capturing PAHs due to its conformational rearrangement to match the molecular structure of PAHs.[28,29] For example, our group recently reported that *homopolymer* vesicles based on poly[2-hydroxy-3-(naphthalen-1-ylamino)propyl methacrylate] (PHNA) effectively adsorbed PAHs by $\pi-\pi$ stacking.[30]

Although PAHs and bacteria are both dangerous, most treatment agents can only remediate one of them. These problems encouraged chemists and materials scientists to develop next-generation treatment agents using new design principles. Herein we designed a novel nanocapsule self-assembled by a *statistical* copolymer, poly[[2-hydroxy-3-(naphthalen-1-ylamino)propyl methacrylate]-*stat*-[2-(*tert*-butylamino)ethyl methacrylate]] [P(HNA$_{23}$-*stat*-TA$_{20}$)]. The

Received: February 23, 2015
Accepted: April 15, 2015
Published: April 17, 2015

DOI: 10.1021/acsmacrolett.5b00142
ACS Macro Lett. 2015, 4, 511−515

nanocapsule can simultaneously inhibit bacteria growth and capture PAHs in water with high efficacy (Scheme 1). The TA

Scheme 1. Formation of P(HNA$_{23}$-*stat*-TA$_{20}$) Statistical Copolymer Nanocapsules for Effective Bacterial Inhibition and PAH Capturing[a]

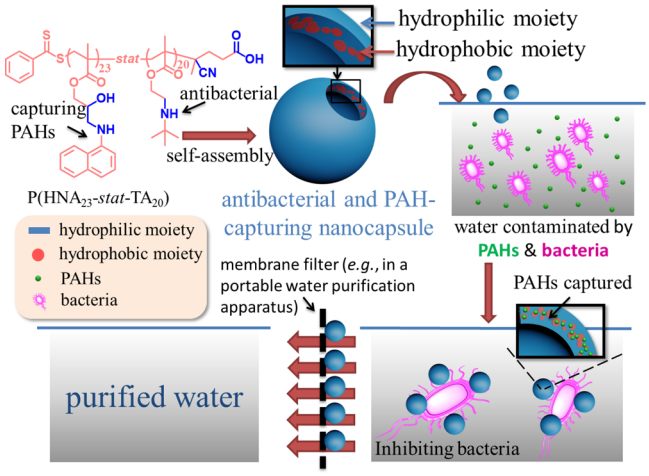

[a]The nanocapsules can effectively inhibit bacteria by a TA unit before filtration to prevent formation of biofilm in the membrane filter. The PAH capturing capacity relies on the $\pi-\pi$ stacking between the PAHs and the naphthalene of HNA in the nanocapsule. The nanocapsules which inhibit bacteria growth and carry the captured PAHs cannot pass through the filter.

segment is designed for inhibiting bacteria growth, while the HNA segment is engineered for capturing PAHs via $\pi-\pi$ interactions with the naphthalene groups in the capsule.

Like homopolymers,[30] statistical copolymers can be easily synthesized in one step and then self-assembled into various nanostructures.[31−33] The P(HNA$_{23}$-*stat*-TA$_{20}$) statistical copolymer was synthesized by a reversible addition−fragmentation chain transfer (RAFT) process according to the synthetic route in Figures S1 and S2 (Supporting Information). First, as shown in Figure S1 (Supporting Information), the HNA monomer was synthesized by ring-opening reaction of glycidyl methacrylate (GMA) by 1-naphthylamine (1-NA). An excess of 1-naphthylamine was used to avoid the possible reaction between the secondary amine groups in the HNA monomer and the epoxy groups in GMA. Then the target P(HNA$_{23}$-*stat*-TA$_{20}$) copolymer was synthesized by a RAFT process (Figure S2, Supporting Information) using the as-prepared chain transfer agent 4-cyanopentanoic acid dithiobenzoate (CPAD). The characterization of HNA and P(HNA$_{23}$-*stat*-TA$_{20}$) by ^{1}H NMR and GPC was provided in Figures S3−S5 in the Supporting Information. The molecular weight of the copolymer is 10 500 Da (calculated from the ^{1}H NMR spectrum), and the ratio of M_w/M_n is 1.77 (determined by GPC). Yield: ∼70%.

The P(HNA$_{23}$-*stat*-TA$_{20}$) copolymer can easily self-assemble into nanocapsules by a solvent switch method. The hollow structure of the nanocapsules is confirmed by scanning electron microscopy (SEM, Figure 1a) and transmission electron microcopy (TEM, Figure 1b). The hollow cave inside the nanocapsule can be observed when looking into the holes in the nanocapsules (nanocapsule 8 in Figure 1a and more nanocapsules in Figure S6 in the Supporting Information). Due to the relatively high flexibility of the partially hydrophilic PTA

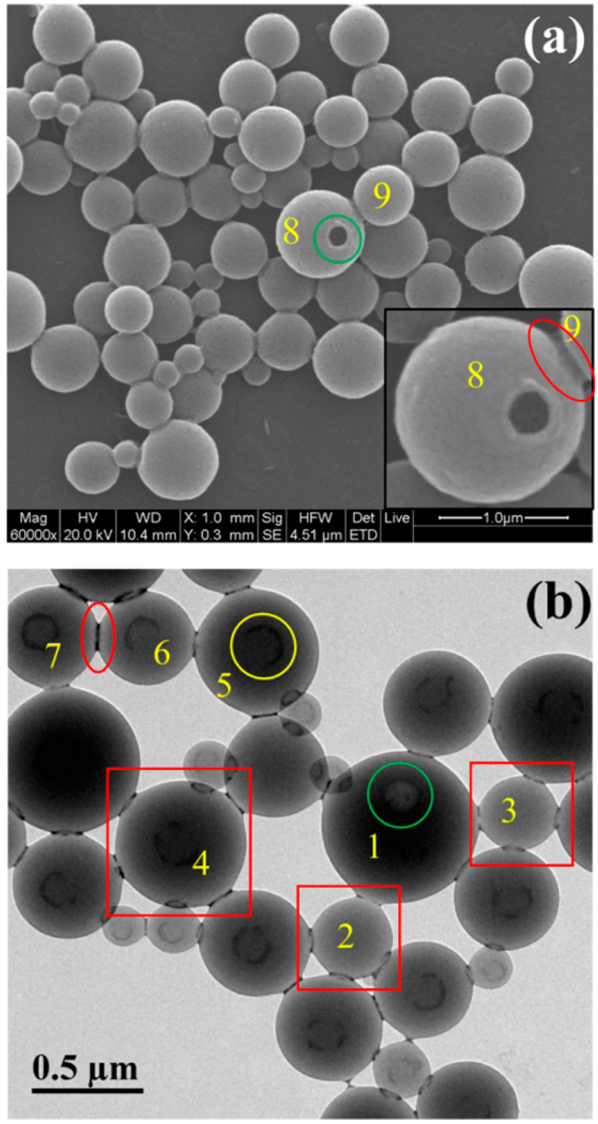

Figure 1. Electron microscopy analysis of P(HNA$_{23}$-*stat*-TA$_{20}$) *statistical* copolymer nanocapsules: (a) SEM images with one open mouth indicating the hollow structure of nanocapsules and (b) TEM images of nanocapsules stained by phosphotungstic acid. The black hole highlighted by the green circle in nanocapsule 1 corresponds to the open mouth in the SEM image (nanocapsule 8). The black ring highlighted by the yellow circle in nanocapsule 5 indicates the contact of nanocapsules with the carbon film substrate. The red areas highlighted by the rectangles and circles (nanocapsules 2, 3, 4, 6, and 7) in the TEM image correspond to the connection of nanocapsules in the SEM image (8 and 9).

moiety on the outside surface,[18] the nanocapsules can be easily stuck together when closely contacted with each other. Nevertheless, it is possible to break this adhesiveness in the subsequent stages such as drying, leading to the formation of an open-mouth-like hole (Figure 2a).[34,35] Also, the spherical morphology in the SEM indicates the rigid membrane of the nanocapsule which prevents it from collapsing under high vacuum.

The open-mouth hole in the SEM image (nanocapsule 8 in Figure 1a) is consistent with the dark ring of nanocapsule 1 in the TEM image, as highlighted by the green circle in Figure 1b. The areas highlighted by red circles and rectangles in the TEM image (nanocapsules 2, 3, 4, 6, and 7) correspond to the

DOI: 10.1021/acsmacrolett.5b00142
ACS Macro Lett. 2015, 4, 511−515

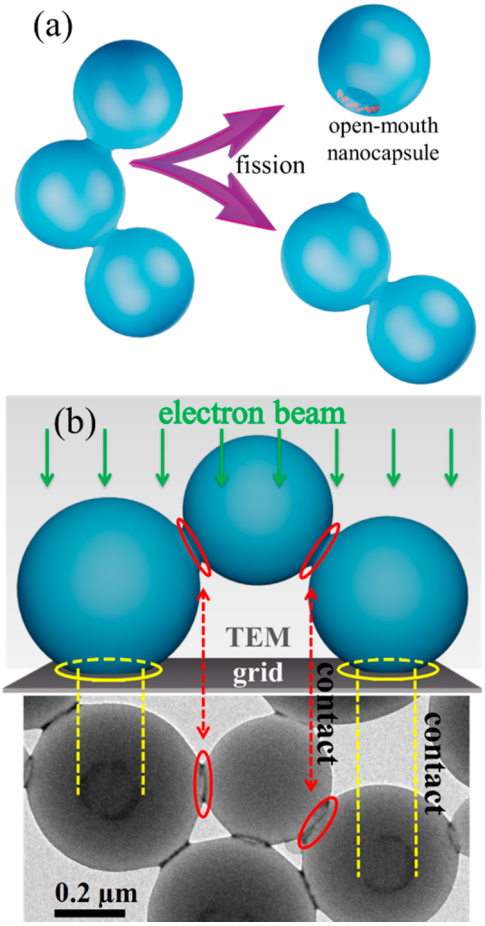

Figure 2. (a) Formation of the open-mouth nanocapsule by the fission of the adhered nanocapsules. The connection between nanocapsules may be broken at the drying stage and then form an open mouth. (b) Illustration of TEM presentations of the contact between adjacent nanocapsules and with the carbon film of the TEM grid. Yellow circles: contact between the bottom of the nanocapsules and the carbon film, resulting in a black ring on the carbon film. Red circles: the contact between adjacent nanocapsules, resulting in the dark ring perpendicular to the carbon film in the TEM image. The nanocapsules in the middle do not have a dark ring due to their stacked up state.

connection of nanocapsules in the SEM image (nanocapsules 8 and 9). The hole highlighted by the yellow circle in nanocapsule 5 in the TEM image indicates the contact of the nanocapsule with the substrate (Figure 2b). Furthermore, the low height to diameter ratio (1/3.5) calculated from the AFM image indicates a hollow structure of the nanocapsule (Figure S7 in the Supporting Information).

It is noteworthy that most of the black rings inside the nanocapsules are due to the contact and slight collapse under gravity on the surface of the TEM grid, which is consistent with the connection between stuck nanocapsules. However, no black ring was observed in nanocapsules 2 and 3 in Figure 1b. This is because both nanocapsules 2 and 3 are supported by four adjacent nanocapsules, which avoid the direct contact of nanocapsules 2 and 3 with the carbon film of the TEM grid (Figure 2b).

The hydrodynamic diameter (D_h) of nanocapsules determined by dynamic light scattering (DLS) is 501 nm with a very low polydispersity index (PDI = μ^2/Γ^2) of 0.033, as shown in Figure 3. The nanocapsules are positively charged in water at

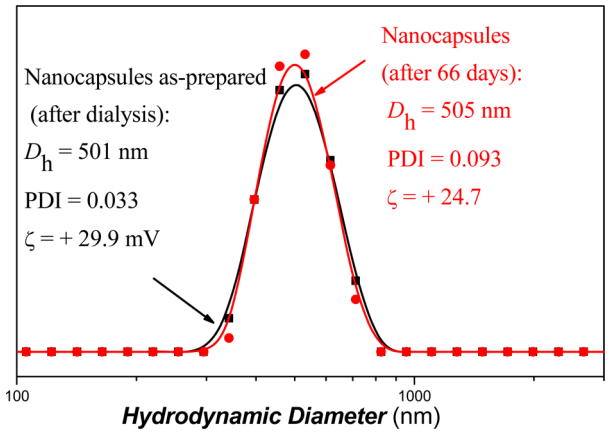

Figure 3. DLS and zeta potential (ξ) results of the P(HNA_{23}-*stat*-TA_{20}) statistical copolymer nanocapsules. The zeta potential was determined at pH 7.0.

pH 7.4 (ξ = +29.9 mV) due to the *tert*-butylamino groups in the TA segment. In addition, the nanocapsules have excellent stability as confirmed by DLS studies since after 66 days the diameter (505 nm) and PDI (0.093) of the redispersed nanocapsules did not change much (Figure 3).

The nanocapsules are useful in water purification due to its bacterial inhibition and PAH capturing capacities. First, to evaluate the antibacterial activity of nanocapsules, *E. coli* and *S. aureus* were selected as typical Gram-negative and Gram-positive bacteria, respectively. The minimum inhibitory concentration (MIC) was used to evaluate the antibacterial activity of the nanocapsules via a broth microdilution method. The MIC is defined as the minimum concentration of an antimicrobial agent at which less than half of the microbes grow compared with the control sample after at least 18 h. Typically, the polymeric nanocapsule solution at different concentrations was placed into each cuvette with microorganism solution. Then the optical density (OD) at 600 nm wavelength of visible light was measured at intervals, as shown in Figure 4. The values of MIC were at 26.19 and 15.52 μM against *E. coli* and *S. aureus*, respectively, showing effective antibacterial activities of nanocapsules. This excellent antibacterial capacity of nanocapsules is related to the cationic character of the TA repeat units of the statistical copolymer with the relative ease of protonation because the pK_a for the conjugate acid form of PTA is relatively high.[36]

To test the PAH capturing capacity of the nanocapsules, fluorescence-quenching experiment was conducted using pyrene as a probe. Figure 5 shows that the as-prepared nanocapsules have excellent capturing capacity toward aromatic compounds. After 6 min, the amount of the residual pyrene decreased in the presence of nanocapsules with various concentrations, indicating that the fluorescence of pyrene in the aqueous solution can be quenched by the nanocapsules. This result confirms that pyrene is successfully captured by the nanocapsules because fluorescent quenching can only occur when the donor and acceptor molecules are sterically close together. Due to the affinities of naphthylamine pendants for polycyclic aromatic compounds through hydrophobic effect and $\pi-\pi$ stacking, the nanocapsules and pyrene tend to get close in the solution. Meanwhile, on the basis of the theory of forster resonance energy transfer (FRET), the partial overlap of the fluorescence emission of pyrene at 360−450 nm and the UV−vis absorbance of naphthylamine at 310−390 nm can be

DOI: 10.1021/acsmacrolett.5b00142
ACS Macro Lett. 2015, 4, 511−515

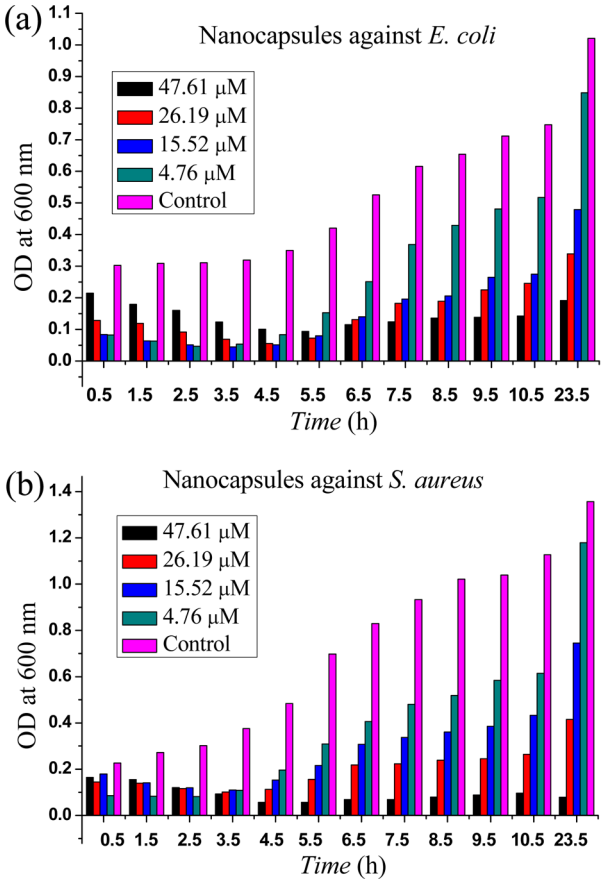

Figure 4. Dose-dependent growth inhibition of bacteria in the presence of P(HNA_{23}-*stat*-TA_{20}) nanocapsules. OD: optical density.

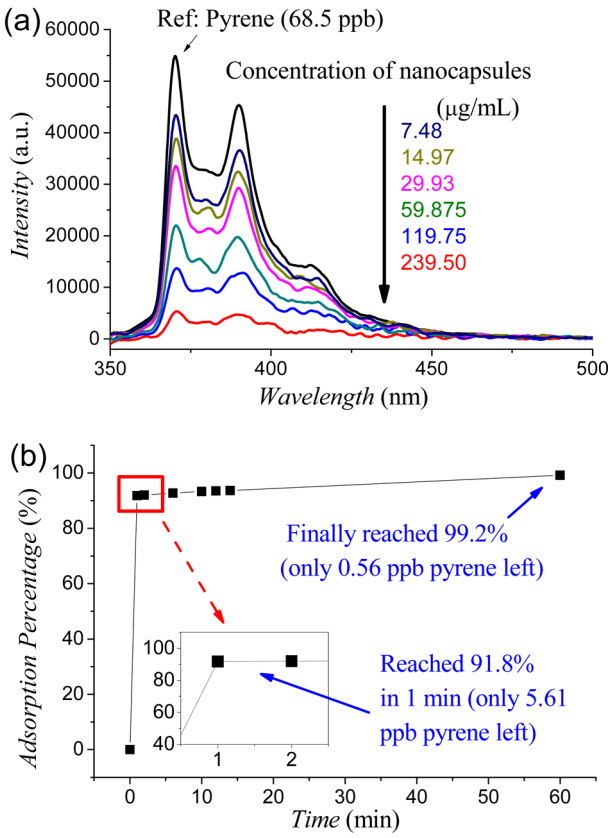

Figure 5. Evidence for $\pi-\pi$ stacking: (a) Fluorescence quenching of pyrene-contaminated water by different concentrations of P(HNA_{23}-*stat*-TA_{20}) nanocapsules. Adsorption results were measured after 6 min. (b) Time dependence of pyrene's adsorption percentage by the nanocapsules at the concentration of 239.50 μg/mL. Conditions: λ_{ex} = 335 nm; $[Pyrene]_{initial}$ = 68.5 ppb. The signal of the control nanocapsule was detracted for each solution.

considered as a donor−acceptor pair. Therefore, the naphthylamine pendant in the P(HNA_{23}-*stat*-TA_{20}) nanocapsules has significant adsorption capability toward aromatic compounds.

The results of the fluorescence quenching test are shown in Figure 5a. The pyrene adsorption kinetics are shown in a time-dependent plot of pyrene's adsorption percentage (Figure 5b). When the P(HNA_{23}-*stat*-TA_{20}) nanocapsules were added, the adsorption percentage of pyrene could reach 91.8% in only 1 min. After 1 h, the adsorption percentage reached 99.2%; i.e., only 0.56 ppb of residual pyrene remained, which was much lower than most of the previously reported systems.[37,38] Also, the efficiency is very high because the nanocapsules could finish the adsorption process in 1 h, which is similar to our recently reported homopolymer vesicles.[30] Therefore, the P(HNA_{23}-*stat*-TA_{20}) nanocapsules are a valuable adsorbent in removing PAHs.

After purification, the nanocapsules can be separated easily. We utilized a simulated PAH and bacteria polluted water which contained pyrene and *E. coli*. The nanocapsules were directly added into the as-prepared polluted water followed by passing a filter membrane with 220 nm of pore diameter. Before filtration, the UV−vis spectra in Figure S9a (Supporting Information) show a high absorbance given by nanocapsules and *E. coli* (but very little for pyrene, see Figure S10a, Supporting Information) in the mixture, while after the filtration, the absorbance was close to zero, indicating that no residues existed in the purified water (Figure S9a, Supporting Information). Similarly, a very high fluorescence intensity of nanocapsules and pyrene (very little for *E. coli*) in the mixture was confirmed by Figure S10b (Supporting Information). It is noteworthy that the fluorescence disappeared after filtration (Figure S9b, Supporting Information). In contrast, the control sample of aqueous pyrene solution still retained high intensity after filtration (Figure S9c, Supporting Information), indicating that only the PAHs captured by nanocapsules could be successfully removed by filtration. Furthermore, the above results are also consistent with the digital photos in Figure S9d (Supporting Information). It is easy to see that the water after filtration is much more transparent than the original solution.

In summary, a novel statistical copolymer was synthesized and self-assembled into a multifunctional nanocapsule (vesicle), which was confirmed by SEM, TEM, AFM, and DLS studies. SEM studies clearly revealed the vesicular structure of nanocapsules with an open-mouth hole. The corresponding TEM analysis revealed the formation mechanism of the open mouth of the nanocapsule and provided people with a new insight for justifying the vesicular structure by TEM (without a classical dark ring in the edge of the vesicle). The nanocapsules can effectively inhibit the bacteria growth in water, which may be used in a water purification system such as a portable apparatus for prolonging its working life by preventing biological contamination. Furthermore, the nanocapsules can remove pyrene in water to an extremely low level (0.56 ppb) in a very short time. The PAH-collected nanocapsules and bacteria can be effectively separated from water by a filter

DOI: 10.1021/acsmacrolett.5b00142
ACS Macro Lett. 2015, 4, 511−515

membrane, showing promising applications in water remediation. Moreover, this rational engineering principle could be extended by statistically copolymerizing HNA with other functional monomers for designing a range of multifunctional nanomaterials, which is ongoing in our lab and will be reported in the future.

■ ASSOCIATED CONTENT

Supporting Information

Materials, synthesis, and characterization (Figures S1−S10). This material is available free of charge via the Internet at http://pubs.acs.org.

■ AUTHOR INFORMATION

Corresponding Author

*E-mail: jzdu@tongji.edu.cn.

Notes

The authors declare no competing financial interest.

■ ACKNOWLEDGMENTS

JD is supported by Shanghai 1000 Plan, Eastern Scholar professorship, and natural science foundation of China (21174107 and 21374080).

■ REFERENCES

(1) Morens, D. M.; Folkers, G. K.; Fauci, A. S. *Nature* **2004**, *430*, 242−249.
(2) Guerrant, R. L.; Steiner, T. S.; Lima, A. A. M.; Bobak, D. A. *J. Infect. Dis.* **1999**, *179*, S331−S337.
(3) Li, Y. M.; Yu, H. S.; Qian, Y. F.; Hu, J. M.; Liu, S. Y. *Adv. Mater.* **2014**, *26*, 6734−6741.
(4) Yuan, H. X.; Chong, H.; Wang, B.; Zhu, C. L.; Liu, L. B.; Yang, Q.; Lv, F. T.; Wang, S. *J. Am. Chem. Soc.* **2012**, *134*, 13184−13187.
(5) Chen, J.; Wang, F. Y. K.; Liu, Q. M.; Du, J. Z. *Chem. Commun.* **2014**, *50*, 14482−14493.
(6) Yuan, H. X.; Liu, Z.; Liu, L. B.; Lv, F. T.; Wang, Y. L.; Wang, S. *Adv. Mater.* **2014**, *26*, 4333−4338.
(7) Lax, A. J. *Nat. Rev. Microbiol.* **2005**, *3*, 343−349.
(8) Lax, A. J.; Thomas, W. *Trends Microbiol.* **2002**, *10*, 293−299.
(9) Ironside, R.; Sourirajan, S. *Water. Res.* **1967**, *1*, 179−180.
(10) Madaeni, S. S. *Water. Res.* **1999**, *33*, 301−308.
(11) Baker, J. S.; Dudley, L. Y. *Desalination* **1998**, *118*, 81−89.
(12) Zhang, J.; Chua, H. C.; Zhou, J.; Fane, A. G. *J. Membr. Sci.* **2006**, *284*, 54−66.
(13) Ignatova, M.; Voccia, S.; Gilbert, B.; Markova, N.; Cossement, D.; Gouttebaron, R.; Jerome, R.; Jerome, C. *Langmuir* **2006**, *22*, 255−262.
(14) Storm, D. R.; Rosenthal, K. S.; Swanson, P. E. *Annu. Rev. Biochem.* **1977**, *46*, 723−763.
(15) Schindler, M.; Osborn, M. J. *Biochemistry* **1979**, *18*, 4425−4430.
(16) Yuan, W. Z.; Wei, J. R.; Lu, H.; Fan, L.; Du, J. Z. *Chem. Commun.* **2012**, *48*, 6857−6859.
(17) Zhang, C.; Zhu, Y. Q.; Zhou, C. C.; Yuan, W. Z.; Du, J. Z. *Polym. Chem.* **2013**, *4*, 255−259.
(18) Zhu, H.; Geng, Q.; Chen, W.; Zhu, Y.; Chen, J.; Du, J. Z. *J. Mater. Chem. B* **2013**, *1*, 5496−5504.
(19) Zhou, C.; Wang, M.; Zou, K.; Chen, J.; Zhu, Y.; Du, J. Z. *ACS Macro Lett.* **2013**, *2*, 1021−1025.
(20) Troisi, G. M.; Bexton, S.; Robinson, I. *Environ. Sci. Technol.* **2006**, *40*, 7938−7943.
(21) Boffetta, P.; Jourenkova, N.; Gustavsson, P. *Cancer, Causes Control* **1997**, *8*, 444−472.
(22) Mahanty, B.; Pakshirajan, K.; Dasu, V. V. *Crit. Rev. Env. Sci. Technol.* **2011**, *41*, 1697−1746.
(23) Wan, D. C.; Chen, F.; Geng, Q. R.; Lu, H.; Willcock, H.; Liu, Q. M.; Wang, F. Y. K.; Zou, K. D.; Jin, M.; Pu, H. T.; Du, J. Z. *Sci. Rep.* **2014**, DOI: 10.1038/srep07296.
(24) Simonich, S. L.; Hites, R. A. *Nature* **1994**, *370*, 49−51.
(25) Beyer, J.; Jonsson, G.; Porte, C.; Krahn, M. M.; Ariese, F. *Environ. Toxicol. Pharmacol.* **2010**, *30*, 224−244.
(26) van der Oost, R.; Beyer, J.; Vermeulen, N. P. E. *Environ. Toxicol. Pharmacol.* **2003**, *13*, 57−149.
(27) Li, D.; Ma, M. *Filtr. Sep.* **1999**, *36*, 26−28.
(28) Kannaiyan, D.; Imae, T. *Langmuir* **2009**, *25*, 5282−5285.
(29) Xie, S. M.; Zhang, M.; Wang, Z. Y.; Yuan, L. M. *Analyst* **2011**, *136*, 3988−3996.
(30) Zhu, Y. Q.; Fan, L.; Yang, B.; Du, J. Z. *ACS Nano* **2014**, *8*, 5022−5031.
(31) Zhu, X. W.; Liu, M. H. *Langmuir* **2011**, *27*, 12844−12850.
(32) Dan, K.; Bose, N.; Ghosh, S. *Chem. Commun.* **2011**, *47*, 12491−12493.
(33) Tian, F.; Yu, Y. Y.; Wang, C. C.; Yang, S. *Macromolecules* **2008**, *41*, 3385−3388.
(34) Vriezema, D. M.; Hoogboom, J.; Velonia, K.; Takazawa, K.; Christianen, P. C. M.; Maan, J. C.; Rowan, A. E.; Nolte, R. J. M. *Angew. Chem., Int. Ed.* **2003**, *42*, 772−776.
(35) Huang, C. S.; Wen, L. P.; Liu, H. B.; Li, Y. L.; Liu, X. F.; Yuan, M. J.; Zhai, J.; Jiang, L.; Zhu, D. B. *Adv. Mater.* **2009**, *21*, 1721−1725.
(36) Morse, A. J.; Dupin, D.; Thompson, K. L.; Armes, S. P.; Ouzineb, K.; Mills, P.; Swart, R. *Langmuir* **2012**, *28*, 11742−11753.
(37) Arkas, M.; Tsiourvas, D.; Paleos, C. M. *Chem. Mater.* **2003**, *15*, 2844−2847.
(38) Arkas, M.; Eleades, L.; Paleos, C. M.; Tsiourvas, D. *J. Appl. Polym. Sci.* **2005**, *97*, 2299−2305.

DOI: 10.1021/acsmacrolett.5b00142
ACS Macro Lett. 2015, 4, 511−515